Pediatric RESEARCH

BASIC SCIENCE ARTICLE

The effects of neuroblastoma and chemotherapy on metabolism, fecal microbiome, volatile organic compounds, and gut barrier function in a murine model

Christoph Castellani[1], Georg Singer[1], Margarita Eibisberger[1], Beate Obermüller[2], Gert Warncke[1], Wolfram Miekisch[3], Dagmar Kolb-Lenz[4], Gregor Summer[1], Theresa M. Pauer[1], Ahmed ElHaddad[1], Karl Kashofer[5] and Holger Till[1]

BACKGROUND: Following transplantation of human neuroblastoma (NB) cells into athymic mice, we investigated the effects of tumor growth and cyclophosphamide (CTX) treatment on systemic metabolism, gut inflammation and permeability, fecal microbiome and volatile organic compounds (VOCs).

METHODS: NB cells (MHH-NB11) were implanted into athymic mice (n=20); 20 healthy mice served as controls (sham). CTX was given to 20 animals (10 NB and 10 sham) after 8 and 9 weeks. Metabolic changes were measured. Ileum samples were obtained for RT-PCR (claudins 2 and 4, occludin, tight junction protein 1) and apoptosis rate determination. Fecal microbiome and VOCs were analyzed. Values were compared to sham animals.

RESULTS: NB caused reduction of adipose tissue, increases of IL-6 and TNF-α, and decreases of TGF-β1 and -β2. Serum FITC-dextrane levels were increased in NB and improved under CTX. Claudin 4 expression was higher in NB versus NB + CTX and sham animals. NB caused increased apoptosis of epithelial cells. NB but also CTX led to a reduction in the abundance of *Lactobacillus*. NB led to alterations of the fecal VOC profile.

CONCLUSIONS: NB caused a catabolic pro-inflammatory state, increased gut permeability, altered fecal VOCs and reductions of *Lactobacillus*. Further investigations are required to determine if modifications of the intestinal microbiome may reverse some of the observed effects.

Pediatric Research (2019) 85:546–555; https://doi.org/10.1038/s41390-019-0283-1

INTRODUCTION

With an incidence of 10.7 per 1 million, neuroblastoma (NB) represents the most common extracranial malignant tumor in children.[1] NB remains distinct from other solid pediatric tumors due to its biological heterogeneity and range of clinical behavior spanning from spontaneous regression to cases of highly aggressive metastatic disease unresponsive to standard and investigational anti-cancer treatment.[1]

The "metabolic competition" for nutrients between host and tumor cells has recently emerged as a promising research area. In this field, the phenomenon of tumor-associated catabolism has gained increasing interest.[2] Malignant tumors may lead to depletion of both adipose and muscle tissue[2] causing significant mortality and morbidity in cancer patients. Although the full picture is rarely seen in children, about one half of pediatric patients with malignant tumors suffer from malnutrition.[3] For instance, stage III and IV NBs are associated with a high risk of undernourishment.[4] Amongst other factors, pro-inflammatory cytokines have been discussed as key players in the pathophysiology of tumor catabolism.[5–7] Additionally, data derived from recent experimental tumor models have revealed an interaction between tumor, metabolism, and the hosts' intestinal microbiota.[7–10]

The intestinal microbiota is composed of a complex community of 100 trillion intestinal archaeal and bacterial cells of more than 1000 different species.[11] These bacteria have a distinct metabolism resulting in the production of metabolites and microbe-associated molecular patterns. Some of these metabolites are secreted in the hosts' stools and are referred to as fecal volatile organic compounds (VOCs). Fecal VOCs reflect the microbial metabolic activity[12] and are held responsible for the characteristic smell of bacteria.[13]

In cases of cancer, bacterial metabolites may influence the patients' nutrient uptake, metabolism, gut motility and barrier function, and systemic inflammatory responses.[14] Consequently, alterations of the intestinal microbial composition associated with increased pro-inflammatory cytokines and a catabolic state have been observed in animal models of leukemia and neuroblastoma.[7,8]

With modern chemotherapy the 5-year survival of patients with NB has increased to 76%.[15] Amongst others, cyclophosphamide (CTX) belongs to the drugs for SIOPN standard (HRNBL1.7/SIOPEN) chemotherapy of NB. Apart from its impact on tumor growth, chemotherapy may also cause disturbed gut barrier function with marked bacterial translocation[16–18] and increased inflammation. Additional to the effect on the bowel wall recent studies have also

[1]Department of Paediatric and Adolescent Surgery, Medical University of Graz, Graz, Austria; [2]Department of Biomedical Research, Medical University of Graz, Graz, Austria; [3]Experimental Research Center, Department of Anaesthesiology and Intensive Care, University of Rostock, Rostock, Germany; [4]Core Facility Ultra-Structure Analysis, Medical University of Graz, Graz, Austria and [5]Institute of Pathology, Medical University of Graz, Graz, Austria
Correspondence: Georg Singer (georg.singer@medunigraz.at)

Received: 9 August 2018 Revised: 28 November 2018 Accepted: 6 January 2019
Published online: 16 January 2019

advocated chemotherapy-induced alterations of the intestinal microbiome.[19] Finally, an intact microbiome seems to be essential for the functioning of CTX chemotherapy—for instance by influencing the reprogramming of myeloid cells in the tumor micro-environment.[20]

At present, there are no investigations addressing the complex interaction of metabolism, microbiome, VOC profile, and gut permeability in solid pediatric tumors and chemotherapy. Therefore, the aim of this study was to assess catabolism, fecal microbiome, fecal VOC profile, and gut barrier function in a murine model of neuroblastoma and CTX chemotherapy.

MATERIALS AND METHODS

Animals

Forty male athymic immunodeficient BALBc:Fox1nu mice were obtained from Envigo Laboratories (Envigo Laboratories, San Pietro al Natiosone, Italy) at an age of 7 weeks. Mice were all subjected to the same housing conditions and were kept as singles in individually ventilated cages under specific pathogen-free conditions. Animals were subjected to a 12 h light and dark cycle. Mice had free access to food and water at all times. All experiments were approved by the veterinary board (BMWFW 66.010/0156-WF/V/3b/2016).

Cell culture

Human NB cells (strand MHH-NB11) were obtained from DSMZ laboratories (Leibnitz Institute DSMZ-German Collection of Microorganisms and Cell Cultures, Braunschweig, Germany, cat. no. ACC157, lot No 5) on 24 March 2017. This cell line was established from a neuroblastoma metastasis at an adrenal site of a 4-year-old white boy in 1986 and expresses neuron-specific enolase and synaptophysin (but neither GFAP nor S-100 protein) and carries a 20-fold amplification of MYCN. Before shipment, cells were negatively tested for *Mycoplasma* by DAPI, microbiological culture, and RNA hybridization assays. For further information on the cell line see https://www.dsmz.de/catalogues/details/culture/ACC-157.html. Detailed description of cell culture protocol is shown in Supplement 1.

Following the 6th passage, cells were diluted to a concentration of 500,000 cells/0.1 ml culture medium.[7]

Tumor inoculation and chemotherapy

After adapting for 1 week, mice received intra-peritoneal anesthesia with 0.05 mg/kg Fentanyl (Fentanyl-Jannsen®, Janssen Pharmaceutical N.V., Beerse, Belgium), 5 mg/kg Midazolam (Midazolam Erwo®, Erwo Pharma GmbH, Brunn/Gebirge, Austria) and 0.5 mg/kg Medetomidine (Domitor®, Orion Pharma GmbH, Vienna, Austria). Mice were rested on temperature controllers under a laminar air flow. After median laparotomy mice received four sub-peritoneal depots at 11, 1, 5, and 7 o'clock. In the tumor groups (NB $n = 10$ and NB + CTX $n = 10$) depots contained 500,000 MHH-NB11 cells in 0.1 ml PBS buffer each; in the control groups (SH, $n = 10$ and SH + CTX, $n = 10$) 0.1 ml PBS buffer per depot only. The laparotomy was closed in double layers using absorbable sutures. After wound closure, narcosis was antagonized by sub-peritoneal injection of 1.2 mg/kg Naloxone (Naloxon®, AmoMed GmbH, Vienna, Austria), 0.5 mg/kg Flumzenile (Anexate®, Roche Austria GmbH, Vienna, Austria), and 2.5 mg/kg Atipamezole (Antisedan®, Orion Pharma GmbH, Vienna, Austria). Post-operative pain medication consisted of subcutaneous injections of 4 mg/kg Carprofen (Rimadyl®, Pfizer Corporation, Vienna, Austria) once daily for 3 days.

For CTX chemotherapy, a solution containing 10 mg/ml CTX was prepared by the institution's pharmacy. Animals of the chemotherapy groups (NB + CTX and SH + CTX) received two intraperitoneal doses 50 mg/kg CTX chemotherapy in postoperative weeks 8 and 9 (one each).

Euthanasia, blood, and organ harvesting

Following 9 weeks of tumor growth, mice were prepared for euthanasia. Sixteen hours before euthanasia, mice were gavage-fed with 500 mg/kg fluorescein-isothiocyanate dextrane (FITC-dextrane®, Sigma-Aldrich Handels GmbH, Vienna, Austria) dissolved at a concentration of 50 mg/ml in PBS buffer. Additionally, two stool samples were obtained. One was stored in an Eppendorf vial at −21 °C for microbiome analysis. The other sample (for VOC analysis) was trimmed to a weight of ~25 mg and then immediately transferred into a 20 ml airtight glass vial (Gerstel GmbH, Germany), stored at 6 °C and sent for VOC analysis by overnight express under constant cooling at 6–8 °C.

For euthanasia, mice were put to general anesthesia as described above. At first, blood was sampled by cardiac puncture. Blood samples were drawn to standard serum vials. The blood was allowed to clot for 30 min and then centrifuged at 10,000 rpm for 10 min. The supernatant serum was removed and split for further investigations. Thereafter, mice were sacrificed by cranio-cervical dislocation. The following solid organs were harvested and weighed: liver, spleen, lungs, and kidneys. Additionally, 3 cm of jejunum (2 cm distal of the gastroduodenal junction), 3 cm of ileum (1 cm oral of the ileo-cecal valve), and 3 cm of colon (1 cm distal to the ileo-cecal valve) were obtained. Finally the gonadal, peri-renal, visceral, and inguinal white adipose tissue (WAT) and the gastrocnemius and soleus muscles were dissected and weighed as previously described.[7] At last, the right tibia was prepared and stored in a 0.1 N sodium hydroxide solution buffered with 1% sodium dodecyl sulfate at 60 °C for 12 h. All solid organs, WAT, and muscle weights were then normed to the animals' tibial length.[21] All samples (organs, stool, and serum samples) were labeled with the mouse ID, blinding the examiners for the experimental group.

Fecal microbiome

To keep the storage time short, DNA extraction for determination of the fecal microbiome was conducted within 2 weeks after sampling. The analysis was conducted by 16S rRNA gene profiling of the variable V1–V2 region as previously described.[7,22] Reads were clustered to Operational Taxonomic Units (OTUs) using the pick_open_reference_otus.py script and uclust algorithm based on the greengenes database (gg_otus-13_8-release) and a 97% identity threshold. OTUs were visualized as OTU tables, taxa summary bar charts, and PCOA plots using the Qiime core microbiome script. Additionally, groupings supplied in the mapping file were tested for statistical significance using the QIIME implementation of the Adonis test and significances of individual bacterial strains were determined applying the Kruskal–Wallis test. In case of global significances, a Mann–Whitney *U*-Test corrected for multiple testing was applied for pairwise group comparison.

Analysis of the fecal VOC profile

For VOC analysis, samples were maintained at a temperature of 6 °C. Measurements were conducted within 48 h after harvesting the samples. VOC were pre-concentrated, detected, and quantified in the headspace of fecal samples by means of solid phase micro extraction (SPME) and gas chromatography-mass-spectroscopy (GC/MS) as described before.[23,24] For preconcentration, a commercially available SPME fiber (carboxen/polymethylsiloxane, Supelco, Bellefonte, PA) was used. An Agilent 7890 A gas chromatograph coupled to an Agilent 5975 C inert XL MSD with triple axis detector was used to separate and detect the volatile organic substances desorbed from the SPME device.

Characterization of the inflammatory response

Serum levels of lipopolysaccharide (LPS) were detected using a commercially available LPS assay kit (Mouse Lipopolysaccharide (LPS) ELISA kit, BlueGene Biotech, Shanghai, China, cat no E03L0268).

A commercially available Luminex® magnetic bead assay (MMHMAG-70K, Merck Chemicals and Life Science GmbH, Vienna, Austria) was configured to detect granulocyte-monocyte colony stimulating factor (GM-CSF), granulocyte colony stimulating factor (G-CSF), macrophage colony stimulating factor (M-CSF), Interleukins (IL) 1α, 1β, 2, 4, 6, and 10, macrophage inflammatory proteins (MIP) 1α, 1β, and 2, monokine induced by gamma-interferon (MIG), interferon gamma (INF-γ), tumor necrosis factor alpha (TNF-α), regulated on activation normal T-cells expressed and secreted (RANTES), and vascular endothelial growth factor (VEGF).

Additionally, a commercially available ELISA kit (TGFBMAG-64K-03, Merck Chemicals and Life Science GmbH, Vienna, Austria) was used to determine transforming growth factors (TGF) β1 and β2 levels. All tests were performed as described in the manufacturers' instructions.

Light microscopy of tumors and intestinal samples, immunofluorescence histology of ileum samples

The tumors and one sample of each intestinal section (ileum, jejunum, and colon) underwent standard histological processing and hematoxylin–eosin staining. The morphology and inflammation in the bowel wall were classified for ileum and colon gut samples as described in the literature.[25]

HOECHST staining was conducted to determine the ratio of apoptotic intestinal epithelial cells in ileal sections. Specimens underwent immune-histological processing followed by staining with HOECHST working solution (HOECHST B2261-25MG, Lot 017K4122, Sigma Aldrich Handels GmbH, Vienna, Austria). For details see Supplement 1. For evaluation, two representative regions were selected for each specimen and two specimens per mouse were evaluated at an enlargement of 200× (about 150 enterocytes/field). The apoptotic cell ratio was determined as percentage of apoptotic nuclei in relation to the total number of enterocytes.

Electron microscopy (ELMI)

Colon and ileum were opened on the anti-mesenterial side. Bowel content was carefully removed by rinsing with physiologic saline solution. Small pieces (5 × 5 mm) of ileum and colon were fixed in 2.5% (wt/vol) glutaraldehyde and 2% (wt/vol) paraformaldehyde in 0.1 M phosphate buffer (pH 7.4) for 2 h. Samples were post-fixed in 2% (wt/vol) osmium tetroxide for 2 h at room temperature, dehydrated in graded series of ethanol and embedded in TAAB (Agar Scientific, Essex, GB) epoxy resin and allowed to polymerize for 48 h at 60 °C. Sections were stained with lead citrate and uranyl acetate. Four samples of ileum and four samples of colon were examined per group by transmission electron microscopy.

Gut permeability assay

Four-hundred microliters of serum per mouse were stored at 6 °C in absolute dark until further evaluation. The standard curve was obtained according to the manufacturer's protocol. The serum FITC-dextrane levels were obtained by photometry at 485 and 535 nm.[26]

Examination of intestinal barrier markers by real-time polymerase chain reaction

Real-time PCR for gut permeability was obtained from ileum sections. Markers (tight junction protein 1, occludin, claudin 2, claudin 4, and CD14) were chosen according to previous reports in the literature.[27] A detailed description of the measurements is given in Supplement 1.

Commercially available kits were used to examine claudin 2 and claudin 4 protein expressions in ileum samples (Blue Gene Mouse claudin 4 ELISA kit ABIN 1745294 and ELISA kit for claudin 2 Cloud Clone Corp. ABIN428288, both obtained through antikörper.online.com). Processing and measurements were conducted as required by the manufacturer. A detailed description of the method is given in Supplement 1.

Statistics

Data were managed with Microsoft Excel 2016® spreadsheets. For statistical analysis, data were transferred to SPSS 22.0®. Nominal and ordinal data are displayed as numbers and percent. Metric data are presented as median and interquartile range (IQR). A detailed report of the statistical methods for microbiome analysis can be found in the literature.[7] Due to the sample size, non-parametric tests (Kruskal–Wallis Test followed by pairwise testing by Mann–Whitney *U*-Test with Bonferroni correction) were used for group comparisons. Additionally, correlation analysis between cytokines, FITC-dextrane levels, and VOC were conducted with a two-sided Spearman Test (the correlation coefficient will be abbreviated with *R*). *p*-values < 0.05 were considered statistically significant.

RESULTS

One mouse of the NB group succumbed postoperatively. One animal in the NB group and one in the NB + CTX group did not develop a tumor. Therefore, 37 animals ($n = 8$ NB, $n = 9$ NB + CTX, $n = 10$ SH, $n = 10$ SH + CTX) were studied. Neuroblastoma was confirmed on standard HE stains in both tumor groups (NB, NB + CTX). Body, tumor, and white adipose tissue weights are displayed in Table 1. Mice of the tumor groups (NB and NB + CTX) presented with depleted adipose tissue with significantly reduced inguinal, gonadal, peri-renal, and total WAT. There was no significant difference regarding the muscle weights. Tumor macroscopy, HE histology and immunohistochemical stainings for GFAP, neurofilament, synaptophysine, and vimentine are shown in Fig. 1.

Fecal microbiome analysis

α-diversity (Chao1 index) of the fecal microbiome was not significantly different between the four groups. Additionally, Shannon Index was 4.92 for NB, 5.13 for NB + CTX, 4.80 for SH, and 5.14 for SH + CTX. There was no significant global difference for the Shannon Index ($p = 1.0$; Kruskal-Wallis-Test).

However, β-diversity was significantly different comparing NB to SH animals ($p = 0.012$, unweighted UniFrac), but not between NB and SH + CTX ($p = 0.085$, unweighted UniFrac) or NB + CTX ($p = 0.687$, unweighted UniFrac) mice. Additionally, there was a significant increase of β-diversity comparing SH to NB + CTX ($p = 0.013$, unweighted UniFrac) but not to SH + CTX ($p = 0.147$, unweighted UniFrac) animals. Finally, there was no significant difference of β-diversity between NB + CTX and SH + CTX groups ($p = 0.130$, unweighted UniFrac).

There were significant global differences between the total OTU reads in the groups ($p = 0.004$; Kruskal–Wallis Test; Fig. 2). The pairwise comparison yielded significantly higher reads for NB compared to SH ($p = 0.004$; Mann–Whitney *U*-Test with Bonferroni correction). Although there were no significant differences of the absolute abundances, the analysis of the relative bacterial abundance showed a significant decrease of *Lactobacillus* genus in NB, NB + CTX, and SH + CTX compared to SH.

Fecal VOC profile

From more than 200 detectable VOC the most predominant 27 different fecal VOC were further analyzed (Table 2). 3-Methylfuran and the aldehydes 2-Methylbutanal, 3-Methylbutanal and 2-Methylpropanal were significantly decreased in tumor animals (NB, NB + CTX) compared to sham groups (SH, SH + CTX). The ketone 2-Hexanone showed an increase in tumor (NB and NB + CTX) compared to sham (SH and SH + CTX) mice.

Cytokines and LPS

The pro-inflammatory cytokines TNF-α and IL-6 were significantly increased in tumor animals (NB and NB + CTX) compared to SH and SH + CTX mice (Table 3). Additionally, there was a significant decrease of IL-1α in tumor animals compared to sham. The

Table 1. Animal and tumor weight (g), muscle and WAT weights normed for tibial length at euthanasia (g/mm)

Item	NB	NB + CTX	SH	SH + CTX	*p*-value
BWT	34.5 (5.8)	31.5 (3.4)	33.6 (2.3)	34.5 (3.5)	0.149
Tumor	3.753 (4.703)	3.022 (3.935)	—	—	0.370
Mm.	0.010 (0.003)	0.010 (0.001)	0.011 (0.002)	0.010 (0.003)	0.061
Inguinal WAT	**0.003 (0.006)**	**0 (0.004)**	**0.008 (0.004)**[a]	**0.006 (0.004)**[a,b]	**<0.001**
Gonadal WAT	**0.009 (0.009)**	**0.005 (0.008)**	**0.015 (0.009)**[b]	**0.016 (0.006)**[b]	**0.001**
Perirenal WAT	**0.002 (0.003)**	**0.002 (0.002)**	**0.005 (0.003)**[a,b]	**0.005 (0.002)**[b]	**0.001**
Visceral WAT	0.007 (0.010)	0.012 (0.006)	0.012 (0.009)	0.015 (0.013)	0.126
Total WAT	**0.026 (0.024)**	**0.019 (0.011)**	**0.043 (0.019)**[b]	**0.040 (0.022)**[a,b]	**<0.001**

Data are displayed as median (IQR)
BWT body weight without tumor, *Mm* gastrocnemius and soleus muscles, *WAT* white adipose tissue
Items with statistically significant differences are highlighted by bold letters
[a]Significant difference vs. NB
[b]Significant difference vs. NB + CTX

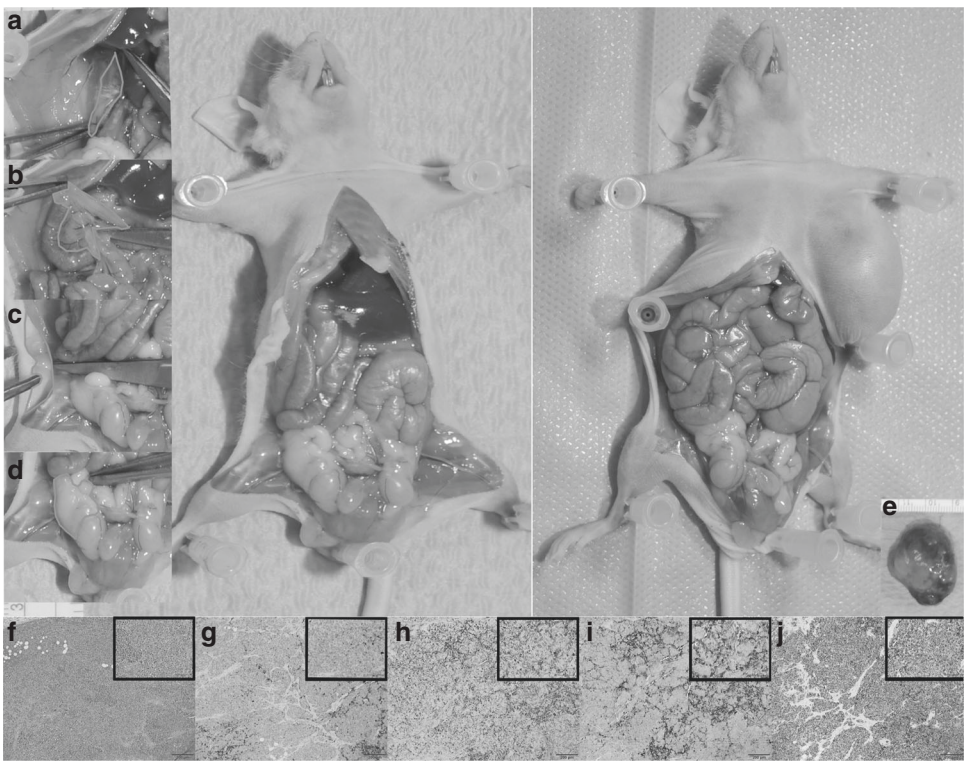

Fig. 1 SH (left) and NB (right) animals. Note the depleted WAT in the NB mouse. Panels **a**–**d** show dissection of the peri-renal (**a**), visceral (**b**), inguinal (**c**), and gonadal (**d**) WAT. Panel **e**: tumor macroscopy. Histology and immunostaining of tumor tissue (**f**–**j**). Panels are 100x magnification, inserts 400x magnification. **f** H&E-staining. Tumor cells stained negative for GFAP (**g**) and positive for neurofilament (**h**), synaptophysine (**i**), and vimentine (**j**)

anti-inflammatory cytokines TGF-β1 and TGF-β2 were significantly decreased in tumor (NB and NB + CTX) and increased in SH + CTX mice compared to SH. LPS levels showed no significant differences ($p = 0.105$; Kruskal–Wallis Test).

Gut barrier function and gut permeability

Serum FITC-dextrane levels were significantly higher in NB than in SH and SH + CTX animals (Fig. 3). There was no significant difference between NB and NB + CTX.

Electron microscopy showed no evident differences regarding open and closed tight junctions between the groups (Fig. 3).

HOECHST staining revealed significant differences in the apoptosis rate between the groups ($p = 0.009$; Kruskal–Wallis Test) (Fig. 3). The apoptosis rate was highest in NB followed by NB + CTX, SH, and SH + CTX. Pairwise comparisons revealed a significant difference between NB and SH + CTX ($p = 0.039$; Mann–Whitney *U*-Test with Bonferroni correction) and a trend between NB and SH ($p = 0.056$; Mann–Whitney *U*-Test with Bonferroni correction).

RT-PCR analysis of the ileum yielded no statistically significant differences for Tjp1, occludin, and claudin 2. Claudin 4 gene expression, however, was significantly higher in NB animals compared to NB + CTX and SH (Fig. 3). Analysis of the protein expression in ileum samples revealed a similar distribution pattern with highest levels of claudin 4 in NB and SH + CTX but without significant global differences. Claudin 2 protein expression showed no significant difference between the groups. The distribution did not resemble the RNA expression.

a

Phylum level	Class level	Order level	Family level	Genus level	NB	NB+CTX	SH	SH+CTX	*p*-value
Actinobacteria					0.008	0.00b*	0.003	0.003**	0.076
	Coriobacteriia	*Coriobacteriales*	*Coriobacteriaceae*	*Adlercreutzia*	7.8×10^{-4}	2.1×10^{-4}*	3.0×10^{-4}	2.5×10^{-4}**	0.075
Bacteroidetes					0.418	0.404	0.407	0.434	0.901
Cyanobacteria					0.001	7.3×10^{-4}*	1.5×10^{-4}	0.002#	0.021
Deferribacteres					0.061	0.053	0.056	0.035	0.480
Firmicutes					0.421	0.453	0.454	0.455	0.917
	Bacilli				0.042	0.030	0.089*,**	0.044#	0.007
		Lactobacillales			0.042	0.030	0.085*,**	0.044#	0.044
			Lactobacillaceae	*Lactobacillus*	0.042	0.030	0.085*,**	0.043#	0.044
Proteobacteria					0.002	4.2×10^{-4}	2.6×10^{-4}	1.4×10^{-4}	0.378
Tenericutes					0.089	0.086	0.078	0.069	0.601

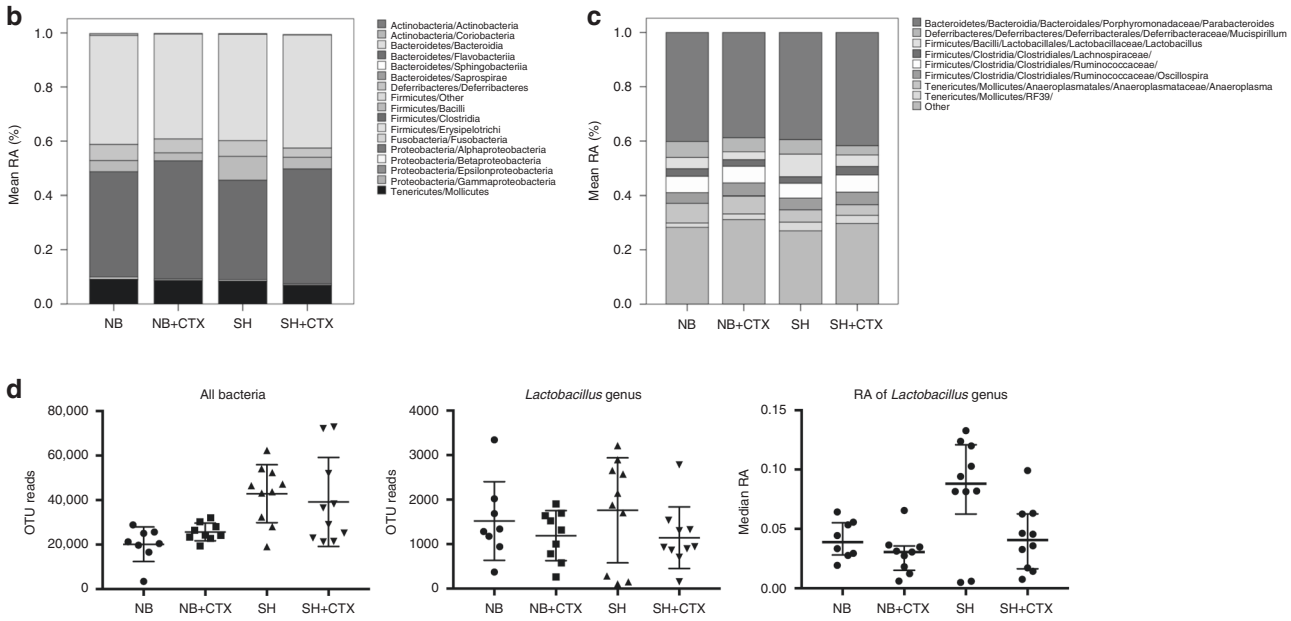

Fig. 2 Fecal microbiome analysis. Panel **a**: mean relative abundances at the different levels; the *p*-value gives global differences assessed by the the Kruskal–Wallis Test; *marks a significant difference compared to NB, **represents a significant difference to NB + CTX and #a significant difference to SH (Mann–Whitney *U*-Test with Bonferroni correction). Panel **b**: mean relative abundances at the class level, especially the decrease of the *Bacilli* class in the groups NB, NB + CTX, and SH + CTX in comparison to SH has to be noted. Panel **c**: mean relative abundances of the different groups at the genus level (only genus with an RA > 2% are displayed). Panel **d**: total OTU reads, OTU reads of *Lactobacillus* genus and relative abundance of *Lactobacillus* genus (median and IQR)

Light microscopy revealed that the total inflammation score (taking epithelial architecture, mucosal architecture, and inflammation into account) was not statistically significantly different between the groups (data are displayed in Supplement 2).

Correlation analysis

The total WAT as marker for catabolism significantly correlated with tumor weight (R −0.675), IL-1α (R 0.380), TNF-α (R −0.326), TGF-β1 (R 0.541), TGF-β2 (R 0.474), 3-Methylfuran (R 0.378), 3-Methylbutanal (R 0.344), 2-Methylbutanal (R 0.337), *Lactobacillus* (R 0.418) and the apoptosis rate (R −0.518).

Regarding the fecal microbiome, *Lactobacillus* significantly correlated with total WAT (R 0.418), IL-1α (R 0.513), TGF-β1 (R 0.327), and Acetic Acid (R −0.407).

A complete overview of correlations giving all significances and correlation coefficients is shown in Supplement 3.

DISCUSSION

In the present study, we sought to unravel the influence of neuroblastoma and chemotherapy with cyclophosphamide on the fecal microbiome and VOC profile, inflammation, and the gut barrier. The tumor model applied was already reported in a previous study by the authors[7] and has achieved tumor take rates of 90%. Cyclophosphamide (CTX) was chosen because it is part of the standard chemotherapy of human neuroblastoma according to SIOPN guidelines. CTX was administered at 50 mg/kg because it has been shown to significantly suppress tumor growth (in a CT26 colon carcinoma model).[28] Additionally, this dosage has been shown to influence the gut permeability in mouse models.[29] The dosage also resembles the treatment of human neuroblastoma.

At euthanasia, the tumor-bearing animals (NB and NB + CTX) exhibited a catabolic state with significant reduction of the total WAT. Chemotherapy with cyclophosphamide even worsened catabolism with a further reduction of adipose tissue mass. In accordance with previous studies, the tumor-associated catabolic state was associated with significant elevations of pro-inflammatory cytokines (TNF-α, IL-6).[7] Alterations of both of these cytokines have been described to cause tumor-associated cachexia[5] and may thus be responsible for the catabolism observed in this investigation. At the same time, we could demonstrate a significant reduction of anti-inflammatory TGF-β1 and -β2 in tumor animals. Cyclophosphamide ameliorated this effect and led to an increase of these anti-inflammatory cytokines in both NB + CTX and SH + CTX. SH + CTX animals demonstrated even higher levels than SH mice suggesting a positive influence of CTX on serum TGF levels. Although there was no difference in endotoxemia (serum LPS levels) bacterial translocation to mesenteric lymph nodes may have occurred but was not assessed in this project. In contrast to previous reports of neuroblastoma-bearing mice[7] and without evident reasons, anti-inflammatory IL-10 showed no changes in the current examinations. Interactions between host, tumor, microbiome, and gut barrier are suspected

Table 2. Fecal volatile organic compounds (VOCs) in parts per billion at euthanasia

Class	VOC (ppb)	NB	NB+CTX	SH	SH+CTX	*p*-value
Hydrocarbons	Butane	7.5 (9.9)	5.6 (3.0)	12.2 (13.7)	12.6 (19.3)	0.076
	Isoprene	18.7 (4.9)	21.8 (5.3)	20.2 (7.4)	21.0 (11.8)	0.548
	Pentane	5.6 (6.8)	6.9 (8.2)	6.2 (8.3)	6.2 (9.1)	0.862
	Octane	15.8 (30.8)	13.9 (11.5)	20.4 (13.0)	16.3 (9.4)	0.266
Cyclic compounds	2-Methylfuran	4.0 (5.2)	3.7 (3.4)	3.2 (1.4)	5.2 (2.8)	0.527
	3-Methylfuran	**5.9 (5.0)**	**5.1 (2.3)**	**9.5 (5.7)**	**11.5 (6.6)**[a]	**0.018**
	2,3,5-Trimethylfuran	11.3 (20.1)	7.5 (7.4)	8.3 (7.8)	7.6 (3.8)	0.362
	Toluene	37.1 (20.0)	23.8 (17.8)	22.9 (16.8)	30.9 (12.2)	0.440
	o-Xylene	11.7 (9.7)	10.3 (6.7)	10.9 (3.6)	10.6 (4.9)	0.900
	Styrene	17.7 (2.5)	16.1 (5.3)	15.7 (3.2)	17.1 (3.6)	0.458
Acids	Acetic Acid	441 (563)	391 (575)	246 (314)	730 (692)	0.128
Alcohols	Ethanol	7658 (6198)	6453 (10,604)	4657 (2379)	9610 (4810)	0.160
Ketones	Acetone	32,474 (29,317)	30,890 (18,899)	21,620 (17,800)	33,126 (25,757)	0.242
	2-Butanon	0(0)	0(0)	0(0)	0 (4222)	0.595
	2,3-Butandion	7810 (6167)	9455 (6343)	6376 (6073)	8631 (5649)	0.671
	3-Pentene-2-one	58.3 (50.0)	27.9 (26.2)	25.5 (48.0)	36.9 (42.0)	0.436
	2-Hexanone	**3.8 (2.5)**	**2.3 (3.4)**	**0 (1.8)**[b]	**0 (2.6)**	**0.018**
	2-Heptanone	10.7 (6.2)	8.8 (6.7)	8.8 (6.7)	10.6 (9.7)	0.773
	Methylvinylketone	25.9 (23.3)	26.9 (35.2)	26.1 (20.3)	25.2 (27.2)	0.825
Aldehydes	Acetaldehyde	5089 (4191)	3414 (2841)	4424 (4562)	6034 (3945)	0.622
	2-Methylbutanal	**117 (257)**	**124 (150)**	**273 (371)**	**415 (353)**[a]	**0.009**
	3-Methylbutanal	**200 (297)**	**175 (102)**	**333 (483)**	**576 (418)**	**0.019**
	Hexanal	28.0 (23.6)	25.0 (10.6)	29.0 (15.3)	32.3 (16.0)	0.057
	2-Methylpropanal	**195 (220)**	**187 (151)**	**282 (293)**	**533 (464)**[a]	**0.012**
	Benzaldehyde	133 (431)	62.7 (88.3)	54.4 (62.9)	65.3 (138)	0.201
Esters	Ethylacetate	45.6 (78.0)	30.6 (59.0)	25.1 (51.4)	49.7 (29.9)	0.923
S-containing	Dimethyldisulfide	0.4 (13.9)	0.5 (2.2)	0 (0.9)	0.9 (1.1)	0.533

Data are displayed as median (IQR)
VOCs with significant differences are printed in bold letters
[a]Significant differences vs. NB + CTX
[b]Significant differences vs. NB

as the main causes for the pro-inflammatory state observed in tumor-bearing animals.

The fecal microbiome analysis showed significant differences in the total OTU reads. In this regard animals of the tumor groups (NB and NB + CTX) had a lower number of reads than SH and SH + CTX. The OTU reads of *Lactobacillus* genus showed no significant differences between the groups. As the total reads were different, this went along with significant changes of the relative abundance in the genus *Lactobacillus*. The 97% threshold for OTU analysis applied in this project allows to differentiate on the genus, but not on the species level. Hence, it was not possible to give exact information about the *Lactobacillus* species concerned in this experiment. In other studies, alterations of *Lactobacillus* have been described in the fecal microbiome of experimental BaF3 leukemia models which have shown that reductions of *L. reuteri* and *L. Johnsonii* were associated with inflammation and increased muscle atrophy.[10] Similarly, we were able to demonstrate that NB causes a significant reduction of the relative abundance of *Lactobacillus* genus together with increased pro- and decreased anti-inflammatory cytokines. We even found a significant correlation of *Lactobacillus* genus with the total WAT (as marker for the catabolism). Additionally, there was a weak correlation with IL-1α and TGF-β2, but not with the other cytokines. At present, there are no other investigations reporting on correlation analysis of bacterial relative abundances and inflammatory markers in tumor animals.

The relative abundance of *Lactobacillus* was not only influenced by NB but also by CTX chemotherapy. In this regard we could demonstrate a significant reduction of *Lactobacillus* in SH + CTX compared to CTX. These changes are in accordance with previous reports demonstrating a direct influence of CTX on *Lactobacillus* as well as gut barrier function.[26] The importance of *Lactobacillus* becomes even more evident as substitution of *Lactobacillus* with restorations of their relative abdundance has been shown to decrease inflammation and reduce tumor progression in murine models of leukemia and bladder cancer.[10,30] Additionally, recent investigations could demonstrate that an intact intestinal microbiome seems to be essential for the effectivity of anti-cancer therapy with CTX, platinum salts and immune-modulators.[20] Taken together, future studies should unravel whether or not anti-cancer treatment can be complemented with restoration of *Lactobacillus* in cases of neuroblastoma.

The epithelial lining of the intestine represents a central part of the gut barrier.[31] It functions as a selective filter for the para- and transcellular transport of liquids, electrolytes and nutrients. Additionally, it forms a protective barrier for bacteria and bacterial toxins.[32,33] Increased gut permeability can either be caused by apoptosis of epithelial cells or by altered porosity of the tight junctions (TJ).[34] TJ are among the most important

Table 3. Inflammatory cytokines, chemokines, and LPS (pg/ml)

Cytokine	NB	NB + CTX	SH	SH + CTX	*p*-value
G-CSF	1080 (900.8)	908.3 (2358)	657.9 (473.2)	1023 (1196)	0.227
GM-CSF	32.1 (69.8)	23.6 (13.7)	0 (10.7)	34.6 (36.7)	0.134
M-CSF	7.7 (32.9)	15.4 (16.9)	0 (10.9)	12.4 (23.4)	0.298
INF-γ	0.5 (5.5)	0 (5.8)	0(0)	0 (2.7)	0.459
TNF-α	**2.6 (3.6)**	**1.7 (2.9)**	**1.2 (0.5)**[a]	**1.5 (1.3)**	**0.012**
IL-1α	**88.5 (215.0)**	**246.1 (153.4)**	**447.7 (364.7)**[a]	**393.2 (470.1)**[a]	**0.007**
IL-1β	0 (6.2)	0 (4.1)	0 (39.7)	0(0)	0.864
IL-2	0(0)	0(0)	0(0)	0(0)	0.997
IL-4	2.0 (4.0)	0 (1.2)	0.3 (3.8)	0 (0.1)	0.151
IL-6	**63.5 (69.1)**	**28.3 (37.6)**	**18.1 (49.1)**	**12.9 (21.4)**[a]	**0.005**
IL-10	4.7 (21.8)	4.2 (5.3)	4.1 (34.5)	4.1 (6.0)	0.967
MIP-1α (CCL3)	79.8 (105)	96.8 (53.6)	0 (55.4)	85.0 (56.1)	0.154
MIP-1β (CCL4)	96.0 (11.8)	87.9 (21.7)	58.3 (67.0)	86.2 (29.9)	0.078
MIP-2 (CXCL2)	187.5 (56.7)	176.3 (83.3)	100.2 (176.3)	182.1 (72.8)	0.125
MIG (CXCL9)	129.1 (186.8)	111.1 (69.5)	151.3 (105.1)	105.0 (45.1)	0.257
RANTES (CCL5)	18.6 (9.2)	17.1 (8.2)	15.3 (22.9)	19.2 (11.8)	0.699
VEGF	19.5 (6.1)	12.0 (15.1)	15.7 (11.5)	14.7 (8.4)	0.184
TGF-β1	**30964 (28401)**	**42332 (11588)**	**59809 (17439)**[a]	**68797 (40106)**[a]	**0.001**
TGF-β2	**1663 (1069)**	**1955 (725.4)**	**2811 (1266)**[a]	**3420 (1969)**[a,b]	**0.002**
LPS	4.5 (3.4)	5.4 (5.4)	3.6 (9.3)	2.3 (3.6)	0.105

Data are displayed as median (IQR)
Cytokines with significant differences are printed in bold letters
[a]Significant differences vs. NB
[b]Significant differences vs. NB + CTX

components granting the integrity of the gut barrier.[35] Claudins represent pivotal parts of TJs and can increase (claudins 2 and 10) or decrease (claudins 1, 3, 4, 8, and 15) gut permeability.[35] In pro-inflammatory conditions, such as tumor-associated catabolism, increased levels of pro-inflammatory cytokines (IL-6 and TNF-α among others) can lead to a NFκB-mediated reduction of claudins 1, 3, 4, 5, 7, and 8 along with an increased expression of claudin 2 resulting in increased TJ porosity.[35] Consequently, there is increased leakage of LPS causing CD14 mediated activation of macrophages and aggravation of the inflammatory response. In contrast, anti-inflammatory TGF-β und IL-10 reverse these changes and restore the integrity of the bowel wall.[35]

In our investigation we were able to demonstrate significantly increased gut permeability (increased serum FITC-dextrane) in tumor animals (NB group). Electron microscopy, however, yielded no visible differences regarding the amount of open TJ between the groups. The analysis of TJ components (TJP-1, occludin and claudin 2) gave no evidence for increased porosity in NB animals. Claudin 4 expression was significantly higher in NB animals, but which would lead to decreased porosity (and thus rules out claudin 4 as a possible cause for intestinal hyperpermeability). Additionally, claudin 4 protein expressions showed the same distribution as RNA samples but without significant differences between the groups. Similarly, claudin 2 protein expression showed no significant difference between the groups. The reason for the discrepancy between claudin 2 RNA and protein expression patterns remains unclear. Overall, the impact of claudin expression (RNA and protein) seems to be of minor impact on the gut permeability in this model. The higher rate of apoptotic epithelial cells in NB animals compared to the other groups can be hypothesized as the most likely reason for the increased FITC levels in this group.

Besides the fecal microbiome and the gut barrier this study also investigated the fecal volatile organic compounds. The fecal VOC represents the total of organic volatile compounds or the "smell" of feces. At present, this is the first study to report the fecal volatile emissions in association with an animal model of a solid pediatric tumor and its chemotherapy. The volatile compounds detected in the feces predominantly result from bacterial metabolism of the intestinal microbiota.[12] Thus, tumor-associated alterations of the intestinal microbiome are hypothesized as most likely cause for the alterations of the fecal VOC profile in this study. We could demonstrate a decrease of 3-Methylfluran, 2-Methylbutanal, 2-Methylpropanal, and 3-Methylbutanal along with an increase of 2-Hexanone in tumor-bearing animals compared to sham (compare Table 2). Examinations of cell cultures have shown decreased levels of the aldehydes 2-Methylbutanal, 3-Methylbutanal, and 2-Methylpropanal in lung carcinoma cells[36,37] and thus similar findings as in our tumor animals. Similar to our results, increased levels of the ketone 2-Hexanone were found in cultures of lung carcinoma cells as well as in the urine of mice transplanted with lung carcinoma.[38] Furthermore, there are reports about increased levels of acetic acid in the urine of patients with esophageal cancer,[39] which also match the findings in our tumor mice. In the correlation analysis (Supplement 3), we could only identify a moderate correlation between the relative abundance of *Lactobacillus* genus in stool samples and acetic acid. The entire intestine is colonized with bacteria and all of them have metabolic activity resulting in VOC production. Thus, the VOCs determined in the stool samples may originate from different bowel segments which have not been grasped by the fecal microbiome analysis performed in the present study. The potential of the fecal VOC profile for disease diagnosis, monitoring of treatment efficacy, and/or diagnosis of tumor recurrence needs to be revealed in further examinations.

Limitations of the present study include the use of an athymic and thus T-cell-deficient mouse model. In contrast to other studies using murine tumor cell lines, we have focused our research on

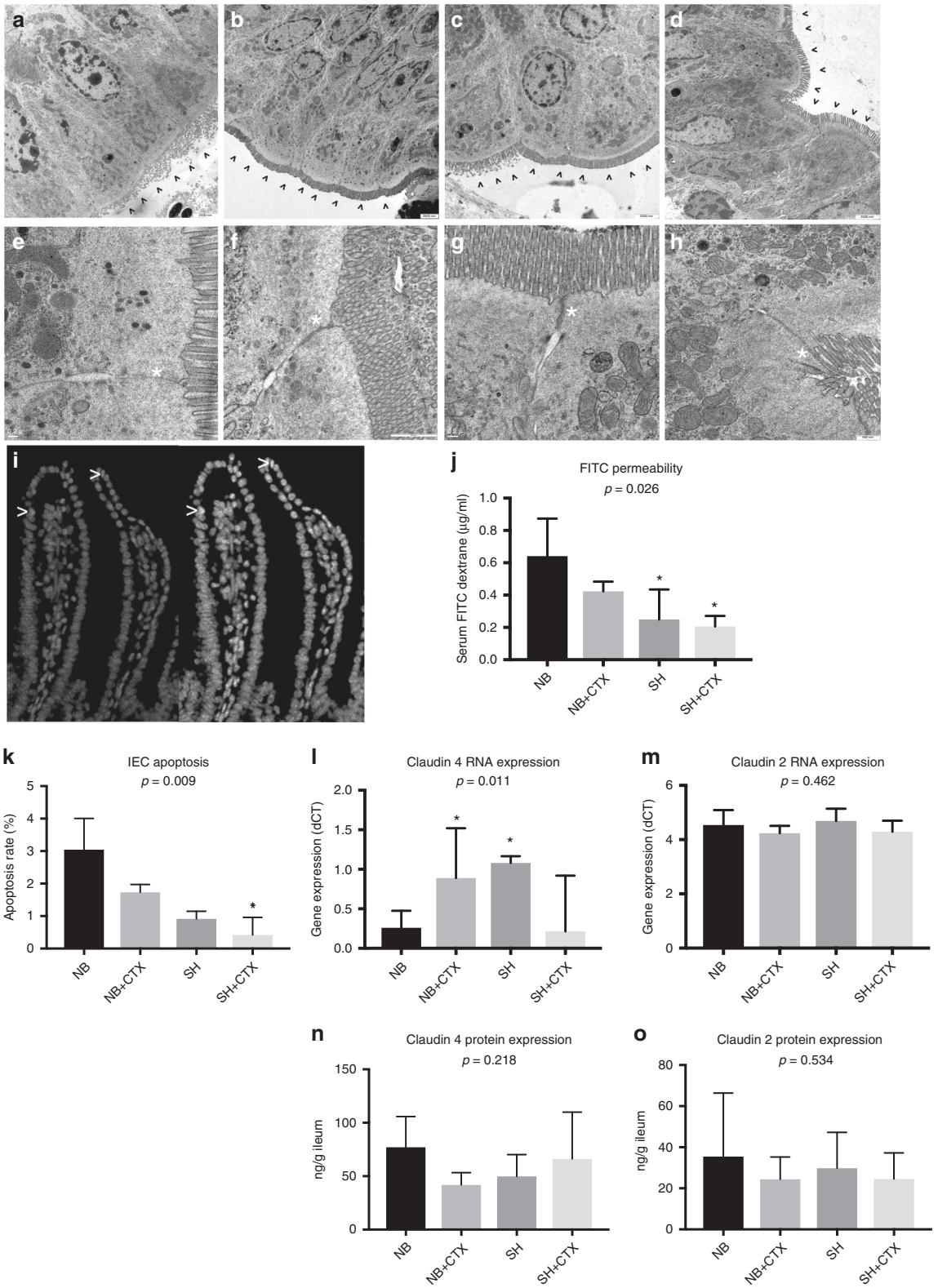

Fig. 3 Gut permeability. Panels **a**–**h**: electron microscopy; NB group (**a**, **e**); NB + CTX (**b**, **f**); SH (**c**, **g**); SH + CTX (**d**, **h**). The top row gives an overview, the bottom row a close-up. The close-up in **e** and **g** shows a closed and that in **f** and **h** an opened tight junction (asterisks). There were no obvious differences regarding closed or open tight junctions between the groups. The arrow heads in the overviews of the top row indicate the luminal microvilli. Panel **i**: HOECHST staining of representative areas in a NB + CTX mouse; >marks apoptotic nuclei. Panel **j**: serum FITC-dextrane levels (bars: median; whiskers: IQR). Panel **k**: apoptosis rate. Panels **l** and **m**: Claudin RNA expression (rtPCR), higher dCT levels represent lower gene expressions (bars: median; whiskers: IQR). **n**, **o** Claudin protein expressions per gram ileum (bars: median; whiskers: IQR). IEC intestinal epithelial cell; * significant difference compared to NB (Mann–Whitney *U*-Test with Bonferroni correction)

the investigation of human tumors. In order to prevent interactions between the host and the tumor caused by the different species an athymic model was chosen. The inflammatory state observed in our tumor animals, however, resembles previous reports on wild-type animals.[8–10] Nevertheless, T-cell-derived cytokines could not be determined in this study. Similar to other researchers,[8,9] the experiments of the present series were only repeated once. Although this is common practice in murine models, it may raise questions regarding the reproducibility of our results. However, our findings are supported by another study group demonstrating lower levels of different *Lactobacillus* strains in their tumor model.[8]

In conclusion, the present study could demonstrate a tumor-induced pro-inflammatory state, decreased *Lactobacillus* genus, and increased gut permeability paired with alterations of the fecal VOC profile in a murine model of human neuroblastoma and its CTX chemotherapy. More data are needed in the field of tumor and chemotherapy-induced alterations of the fecal VOC profile.

ACKNOWLEDGMENTS

The authors thank Anna Kuesz for her great contribution in this investigation. This project was funded by the Monika Kutzner Foundation, the MEFO Graz and the City of Graz.

AUTHOR CONTRIBUTIONS

Christoph Castellani: organized the funding, planned the project, helped collect samples, and wrote the manuscript. Georg Singer: helped with sampling, performed statistical analysis, and helped to write the manuscript. Margarita Eibisberger: performed cell culture and culture diagnostics, helped with measurements and critically reviewed the paper. Beate Obermüller: cared for the animals, helped with sampling and experiments and critically reviewed the manuscript. Gert Warncke: helped with VOC sampling and critically reviewed the manuscript. Wolfram Miekisch: performed VOC analysis and statistics, critically reviewed the manuscript. Dagmar Kolb-Lenz: performed sample preparation and investigations of TEM, critically reviewed the manuscript. Gregor Summer: helped with animal care and sampling at euthanasia, performed conventional histology and analysis, critically reviewed the manuscript. Theresa M. Pauer: helped with sampling and animal care, performed and evaluated immune histology, critically reviewed the manuscript. Ahmed ElHaddad: helped with data management sampling and critically reviewed the manuscript. Karl Kashofer: performed microbiome analysis and statistics, critically reviewed the manuscript. Holger Till: supervised the experiments and critically reviewed the manuscript. All of the authors listed above approved the final version of the manuscript before re-submission after addressing the reviewers' comments.

ADDITIONAL INFORMATION

The online version of this article (https://doi.org/10.1038/s41390-019-0283-1) contains supplementary material, which is available to authorized users.

Competing interests: The authors declare no competing interests.

Publisher's note: Springer Nature remains neutral with regard to jurisdictional claims in published maps and institutional affiliations.

REFERENCES

1. Park, J. R., Eggert, A. & Caron, H. Neuroblastoma: biology, prognosis, and treatment. *Hematol. Oncol. Clin. North Am.* **24**, 65–86 (2010).
2. Al-Zhoughbi, W. et al. Tumor macroenvironment and metabolism. *Semin Oncol.* **41**, 281–295 (2014).
3. Sala, A., Pencharz, P. & Barr, R. D. Children, cancer, and nutrition--A dynamic triangle in review. *Cancer* **100**, 677–687 (2004).
4. Bauer, J., Jurgens, H. & Fruhwald, M. C. Important aspects of nutrition in children with cancer. *Adv. Nutr.* **2**, 67–77 (2011).
5. Argiles, J. M., Busquets, S., Garcia-Martinez, C. & Lopez-Soriano, F. J. Mediators involved in the cancer anorexia-cachexia syndrome: past, present, and future. *Nutrition* **21**, 977–985 (2005).
6. Till, H., Schlichting, N., Oberbach, A. Tumor-associated energy homeostasis: hepatoblastoma and neuroblastoma affect glucose and lipid metabolism as well as ghrelin, GLP-1, and PYY in nude rats. *Eur. J. Pediatr. Surg.* https://doi.org/10.1055/s-0034-1386640 (2014).
7. Castellani, C., et al. Neuroblastoma causes alterations of the intestinal microbiome, gut hormones, inflammatory cytokines, and bile acid composition. *Pediatr. Blood Cancer* **64** https://doi.org/10.1002/pbc.26425 (2017).
8. Bindels, L. B. et al. Restoring specific lactobacilli levels decreases inflammation and muscle atrophy markers in an acute leukemia mouse model. *PLoS One* **7**, e37971 (2012).
9. Bindels, L. B. et al. Non digestible oligosaccharides modulate the gut microbiota to control the development of leukemia and associated cachexia in mice. *PLoS One* **10**, e0131009 (2015).
10. Bindels, L. B. et al. Gut microbiota-derived propionate reduces cancer cell proliferation in the liver. *Br. J. Cancer* **107**, 1337–1344 (2012).
11. Qin, J. et al. A human gut microbial gene catalogue established by metagenomic sequencing. *Nature* **464**, 59–65 (2010).
12. Sagar, N. M., Cree, I. A., Covington, J. A. & Arasaradnam, R. P. The interplay of the gut microbiome, bile acids, and volatile organic compounds. *Gastroenterol. Res Pract.* **2015**, 398585 (2015).
13. Bos, L. D., Sterk, P. J. & Schultz, M. J. Volatile metabolites of pathogens: a systematic review. *PLoS Pathog.* **9**, e1003311 (2013).
14. Ha, C. W., Lam, Y. Y. & Holmes, A. J. Mechanistic links between gut microbial community dynamics, microbial functions and metabolic health. *World J. Gastroenterol.* **20**, 16498–16517 (2014).
15. Coughlan, D., Gianferante, M., Lynch, C. F., Stevens, J. L. & Harlan, L. C. Treatment and survival of childhood neuroblastoma: Evidence from a population-based study in the United States. *Pediatr. Hematol. Oncol.* 1–11 https://doi.org/10.1080/08880018.2017.1373315 (2017).
16. Song, D. et al. Green fluorescent protein labeling *Escherichia coli* TG1 confirms intestinal bacterial translocation in a rat model of chemotherapy. *Curr. Microbiol.* **52**, 69–73 (2006).
17. Green, S. I. et al. Murine model of chemotherapy-induced extraintestinal pathogenic *Escherichia coli* translocation. *Infect. Immun.* **83**, 3243–3256 (2015).
18. Viaud, S. et al. Why should we need the gut microbiota to respond to cancer therapies? *Oncoimmunology* **3**, e27574 (2014).
19. Montassier, E. et al. Pretreatment gut microbiome predicts chemotherapy-related bloodstream infection. *Genome Med.* **8**, 49 (2016).
20. Viaud, S. et al. Gut microbiome and anticancer immune response: really hot Sh*t! *Cell Death Differ.* **22**, 199–214 (2015).
21. Das, S. K. et al. Adipose triglyceride lipase contributes to cancer-associated cachexia. *Science* **333**, 233–238 (2011).
22. Gorkiewicz, G. et al. Alterations in the colonic microbiota in response to osmotic diarrhea. *PLoS One* **8**, e55817 (2013).
23. Bergmann, A. et al. In vivo volatile organic compound signatures of Mycobacterium avium subsp. paratuberculosis. *PLoS One* **10**, e0123980 (2015).
24. Miekisch, W., Trefz, P., Bergmann, A. & Schubert, J. K. Microextraction techniques in breath biomarker analysis. *Bioanalysis* **6**, 1275–1291 (2014).
25. Erben, U. et al. A guide to histomorphological evaluation of intestinal inflammation in mouse models. *Int. J. Clin. Exp. Pathol.* **7**, 4557–4576 (2014).
26. Viaud, S. et al. The intestinal microbiota modulates the anticancer immune effects of cyclophosphamide. *Science* **342**, 971–976 (2013).
27. Buchheister, S. et al. CD14 plays a protective role in experimental inflammatory bowel disease by enhancing intestinal barrier function. *Am. J. Pathol.* **187**, 1106–1120 (2017).
28. Tongu, M., Harashima, N., Tamada, K., Chen, L. & Harada, M. Intermittent chemotherapy can retain the therapeutic potential of anti-CD137 antibody during the late tumor-bearing state. *Cancer Sci.* **106**, 9–17 (2015).
29. Yang, J., Liu, K. X., Qu, J. M. & Wang, X. D. The changes induced by cyclophosphamide in intestinal barrier and microflora in mice. *Eur. J. Pharmacol.* **714**, 120–124 (2013).
30. Seow, S. W. et al. Lactobacillus rhamnosus GG induces tumor regression in mice bearing orthotopic bladder tumors. *Cancer Sci.* **101**, 751–758 (2010).
31. van Vliet, M. J. et al. Chemotherapy treatment in pediatric patients with acute myeloid leukemia receiving antimicrobial prophylaxis leads to a relative increase of colonization with potentially pathogenic bacteria in the gut. *Clin. Infect. Dis.* **49**, 262–270 (2009).
32. Blikslager, A. T., Moeser, A. J., Gookin, J. L., Jones, S. L. & Odle, J. Restoration of barrier function in injured intestinal mucosa. *Physiol. Rev.* **87**, 545–564 (2007).
33. Podolsky, D. K. Mucosal immunity and inflammation. V. Innate mechanisms of mucosal defense and repair: the best offense is a good defense. *Am. J. Physiol.* **277**, G495–G499 (1999).
34. Zeissig, S. et al. Changes in expression and distribution of claudin 2, 5 and 8 lead to discontinuous tight junctions and barrier dysfunction in active Crohn's disease. *Gut* **56**, 61–72 (2007).

35. Gunzel, D. & Yu, A. S. Claudins and the modulation of tight junction permeability. *Physiol. Rev.* **93**, 525–569 (2013).
36. Filipiak, W. et al. Release of volatile organic compounds (VOCs) from the lung cancer cell line CALU-1 in vitro. *Cancer Cell Int.* **8**, 17 (2008).
37. Sponring, A. et al. Release of volatile organic compounds from the lung cancer cell line NCI-H2087 in vitro. *Anticancer Res.* **29**, 419–426 (2009).
38. Hanai, Y. et al. Analysis of volatile organic compounds released from human lung cancer cells and from the urine of tumor-bearing mice. *Cancer Cell Int.* **12**, 7 (2012).
39. Huang, J. et al. Selected ion flow tube mass spectrometry analysis of volatile metabolites in urine headspace for the profiling of gastro-esophageal cancer. *Anal. Chem.* **85**, 3409–3416 (2013).